1   **Simultaneous analysis of antigen-specific B and T cells after SARS-CoV-2**

2   **infection and vaccination**

3

4   **Krista L. Newell[1], Mitchell J. Waldran[1], Stephen J. Thomas[1, 2], Timothy P. Endy[1],**
5   **and Adam T. Waickman[1, 2*]**
6

7   [1]Department of Microbiology and Immunology, SUNY Upstate Medical University,
8   Syracuse, New York, United States of America

9   [2]Institute for Global Health and Translational Science, SUNY Upstate Medical
10   University, Syracuse, New York, United States of America

11   * Corresponding author

12   E-mail: waickmaa@upstate.edu (ATW)

13   Running headline: Co-analysis of antigen-specific lymphocytes

15   Address correspondence and reprint requests to Dr. Adam Waickman, Upstate Medical
16   University, 766 Irving Avenue, Syracuse, NY 13210; email: waickmaa@upstate.edu

17

18   **Abstract**

19   Conventional methods for quantifying and phenotyping antigen-specific lymphocytes

20   can rapidly deplete irreplaceable specimens. This is due to the fact that antigen-specific

21   T and B cells have historically been analyzed in independent assays each requiring

22   millions of cells. A technique that facilitates the simultaneous detection of antigen-

23   specific T and B cells would allow for more thorough immune profiling with significantly

24   reduced sample requirements. To this end, we developed the B And T cell Tandem

25   Lymphocyte Evaluation (BATTLE) assay, which allows for the simultaneous

26   identification of SARS-CoV-2 Spike reactive T and B cells using an optimized Activation

27   Induced Marker (AIM) T cell assay and dual-color B cell antigen probes. Using this

28   assay, we demonstrate that antigen-specific B and T cell subsets can be identified

29   simultaneously using conventional flow cytometry platforms and provide insight into the

30   differential effects of mRNA vaccination on B and T cell populations following natural

31   SARS-CoV-2 infection.

32

33

34   Keywords: SARS-CoV-2, spike protein, vaccination, natural infection, B cells, T cells,

35   antigen-specific

36

Introduction

The identification, quantification, and characterization of antigen-specific lymphocytes is a critical prerequisite for understanding the breadth, magnitude, and functional potential of vaccine and/or natural pathogen-elicited immunity. Multiple distinct methodologic approaches have been developed that allow for the identification of antigen-specific T and B cells. For the identification of antigen-specific T cells, these include quantification of functional cytokine-producing T cells by ELISPOT, flow cytometric detection of intracellular cytokine production following peptide stimulation, staining with peptide/HLA probes, and upregulation of activation-induced markers following antigen engagement (Altman et al., 1996; Kern et al., 2000; Maecker et al., 2001; Frentsch et al., 2005; Dan et al., 2016, 2021). Analogous approaches have also been developed for the identification of antigen specific B cells including, but not limited to, B cell ELISPOT assays and the use of fluorescently conjugated protein probes to stain antigen-specific B cells (Julius et al., 1972; Czerkinsky et al., 1983; Moody and Haynes, 2008; Boonyaratanakornkit and Taylor, 2019). However, a major limitation of the approaches developed thus far is that they interrogate rare B and T cell subsets in isolation. An approach capable of identifying and phenotyping antigen-specific B cells, CD4$^+$ T cells, and CD8$^+$ T cells simultaneously would not only preserve valuable samples by performing multiple assays in parallel, but would also permit the efficient longitudinal assessment of B and T cells that recognize the same antigen over time as they expand and contract following challenge.

59   In this study, we endeavored to simultaneously identify and characterize SARS-

60   CoV-2 spike protein-specific B cells, CD4$^+$ T cells, and CD8$^+$ T cells in the same PBMC

61   sample. We used the combination of an optimized Activation-Induced Marker (AIM)

62   assay to identify spike reactive T cells following stimulation with overlapping spike

63   peptide pools, and spike reactive B cells by baiting with dual spike trimer fluorescent

64   tetramers. This approach was then used to quantify and longitudinally track the T and B

65   cell populations induced by natural SARS-CoV-2 infection and subsequent SARS-CoV-

66   2 mRNA vaccination in the same individuals. Flow cytometric analysis of these antigen-

67   specific populations revealed that while the spike-specific B cell, and to lesser degree

68   CD8$^+$ T cell responses, were consistently enhanced by mRNA vaccination, a clear

69   boosting effect on spike-specific CD4$^+$ T cells was only detectable in individuals with low

70   or undetectable T cell responses following natural infection. Furthermore, we validated

71   our observations of SARS-CoV-2-specific B cell functional enhancement upon

72   vaccination with paired serological analysis. Our findings suggest divergent patterns of

73   B and T cell subset mobilization with repeated antigen encounter and highlight the utility

74   of examining these populations in concert.

75

76

Materials and Methods

Study design. PBMC and sera for this study were obtained from the previously described SUNY Upstate Medical University Convalescent COVID-19 Plasma Donor protocol (Fang et al., 2021; Newell et al., 2021). A subset of 10 donors was selected for focused analysis in the study using the following criteria: 1) blood collection at least 30 days after but not longer than 75 days after their last COVID-19 symptom, 2) immunization with two doses of a SARS-CoV-2 mRNA vaccine at least 9 months after a negative PCR test (8/10 Pfizer-BioNTech, 2/10 Moderna mRNA-1273), and 3) blood collection at least 30 days, but not longer than 22 weeks following vaccination. One subject was excluded from the final analysis due to immunosuppressive treatment for autoimmune disease at the time of sample collection. Archived sera and PBMC from healthy individuals collected prior to December 2019 were used as negative controls. Sample size was determined based on subject availability and conformity of sample collection to the described timeline.

Spike tetramer generation. Full-length SARS-CoV-2 Spike (2P-stabilized, C-terminal Histidine/Avi-tagged) was obtained from BEI resources (Manassas, VA, USA, Cat. NR53524) and biotinylated using a BirA ubiquitin ligase (Avidity, Aurora, CO, USA, Cat. Bir500A) following the manufacturer's recommended protocol. Biotinylated spike protein was purified using a 40K MWCO 2 mL Pierce Zeba™ desalting column (Thermo Fisher Scientific, Waltham, MA, USA, Cat. 87768), and mixed with streptavidin BV421 (BD, Cat. 563259) or streptavidin allophycocyanin (APC) (BD Cat. 554067) separately at a 20:1 ratio (~6:1 molar ratio) as previously described (Dan et al., 2021). Tetramerized

100   Spike probes were stored at 4°C until use. Just prior to probe staining, spike protein

101   probes were added one-by-one to FACS wash buffer (1x PBS, 2% fetal bovine serum)

102   containing 5µM free d-biotin (Avidity, Cat. Bir500A). Both streptavidin-fluor conjugates

103   were used to stain DMSO control samples to further verify the absence of significant

104   frequencies of non-specific streptavidin-binding B cells.

105

106   **Activation Induced Marker (AIM) assay.** Spike-specific T cells were quantitated as a

107   frequency of AIM$^+$ (OX40$^+$CD69$^+$) CD4$^+$ T or (CD25$^+$CD69$^+$) CD8$^+$ T cells among PBMC

108   following 24 hours of stimulation with overlapping peptide pools covering the length of

109   SARS-CoV-2 spike peptide (BEI, Cat. NR52402), as previously described (Fang et al.,

110   2021). Cryopreserved PBMC were thawed, washed twice, and cultured in complete cell

111   culture media: RPMI 1640 medium (Corning, Tewksbury, MA, USA, Cat. 10-040-CV)

112   supplemented with 10% heat-inactivated fetal bovine serum (Corning, Cat. 35-010-CV),

113   1% L-glutamine (Lonza, Basel, Switzerland, Cat. BW17-605E), and 1%

114   Penicillin/Streptomycin (Gibco, Waltham, MA, USA, Cat. 15140122). Cellular viability

115   was assessed by trypan blue exclusion and cells were resuspended at a concentration

116   of 5×10^6 cells/mL. Next, spike peptide pool cocktail was added to each well, diluted to

117   a final concentration of 1 µg/mL/peptide (DMSO concentration 0.5%). Incubation with an

118   equimolar amount of DMSO (0.5%) was used as a negative control, or monoclonal anti-

119   human CD3 (Mabtech, Sweden, Cat. 3420-2AST-10) at a 1:1000 dilution for positive

120   control wells. Cells were cultured for 24 hours at 37°C, 5% CO_2 in polystyrene plates.

121

122   **Staining and Flow Cytometry.** Stimulated PBMC were washed twice in warm

123   complete culture media and transferred to polypropylene 96-well plates for staining in

124   the dark with 50µL of spike tetramer probe cocktail containing 100ng Spike per probe

125   (total 200ng) at 4°C for 1 hour prior to surface staining in FACS wash buffer with the

126   antibodies listed in table S1 at 4°C for 30min. Cells were washed with 1x PBS to avoid

127   binding of antibodies to viability dye and stained with the LIVE/DEAD Fixable Aqua

128   Stain Kit (Thermo, Cat. L34957) in 1x PBS at 4°C for 30min to exclude dead cells. The

129   cells were washed again with FACS buffer to quench remaining dye. Single-color

130   compensation controls were prepared using Onecomp eBeads™ compensation beads

131   (Thermo, Cat. 01111142) and Arc™ Amine Reactive Compensation Bead Kit (Thermo,

132   Cat. A10628) according to manufacturer's instructions. For streptavidin-fluorophore

133   compensation, biotin anti-human CD19 (BioLegend, San Diego, CA, USA, Cat. 302203)

134   was used as a primary stain. Stained cells and compensation controls were acquired on

135   a BD Fortessa or Aria II and analyzed using FlowJo (BD), version 10.8.0. The antibody

136   panel utilized in all experiments is shown in table S2. Validation was performed between

137   batches of spike tetramer probes on the same sample to confirm consistency of binding

138   and fluorescence properties.

139   The frequency of spike-specific B cells was expressed as a percentage of total B

140   cells (CD19$^+$, CD3$^/$CD14/CD56$^/$LIVE/DEAD$^-$, lymphocytes), or as number per

141   10^6 PBMC. Spike-specific CD4$^+$ and CD8$^+$ T cell quantities were calculated as

142   background (DMSO) subtracted data.

143

144   **ELISA.** SARS-CoV-2 Spike/RBD and nucleocapsid antibody titers were quantified using

145   a sandwich ELISA protocol. In brief, 96 well NUNC MaxSorb flat-bottom plates were

146   coated with 3.99 µg/ml recombinant SARS-CoV-2 Wuhan-Hu-1 spike RBD protein (Sino

147   Biological, Beijing, PR China, Cat. 40592-V08B), 1 µg/ml SARS-CoV-2 Wuhan-Hu-1

148   nucleocapsid protein (Sino, Cat. 40588-V08B), 0.15 µg/mL SARS-CoV-2 alpha variant

149   spike RBD protein (BEI, Cat. NR-54004), or 0.15 µg/mL beta variant spike RBD protein

150   (BEI, Cat. NR-55278) diluted in sterile 1x PBS. Plates were washed and blocked for 30

151   min. at RT with 0.25% BSA + 1% Normal Goat Serum in 0.1% PBST after overnight

152   incubation 4°C. Serum samples were heat-inactivated for 30 min. at 56°C and serially

153   diluted 4-fold eight times starting at 1:200 prior to incubation for 2 hrs. at RT on the

154   blocked plates. Plates were washed and antigen-specific antibody binding was detected

155   using anti-human IgG HRP (MilliporeSigma, St. Louis, MO, USA, Cat. SAB3701362), or

156   anti-human IgM HRP (SeraCare, Milford, MA, USA, Cat. 5220-0328). Secondary

157   antibody binding was quantified using the Pierce TMB Substrate Kit (Thermo, Cat.

158   34021) and Synergy HT plate reader (BioTek, Winooski, VT). Antibody binding data

159   were analyzed by nonlinear regression (One site specific binding with Hill slope) to

160   determine EC50 titers, reported as Kd values, in GraphPad Prism 9.1.0 (GraphPad

161   Software, La Jolla, CA). End-point titers of SARS-CoV-2 antigen-reactive serum

162   samples were determined as the reciprocal of the final dilution at which the optical

163   density (OD) was greater than 2x of control SARS-CoV-2 naïve serum.

164

165   **Statistical analyses.** Statistical analyses were performed using Prism version 9.1.0

166   (GraphPad), except for correlations. Spearman's rho rank correlation coefficients were

167   computed in R (version 1.3.1093) using the rcorr function in the Hmisc package

168   (version 4.4-1). Statistical significance was represented as shown: ns: $p > 0.05$, *: $p <$

169   0.05, **: $p < 0.01$, ***: $p < 0.001$, and ****: $p < 0.0001$. Individual analyses performed

170   and sample size (n) are indicated in the figure legend. Statistical tests were chosen

171   based on descriptive statistics for the specified dataset. The column in each column plot

172   indicates the arithmetic mean of the dataset.

173

174   **Study approval**

175   All participants provided written informed consent prior to participation in the study,

176   which was performed according to protocols approved by the Institutional Review Board

177   (IRB) of the SUNY Upstate Medical University under IRB number 1587400 for

178   experimental samples and 1839296-1 for pre-pandemic control samples. All clinical

179   investigation was conducted according to Declaration of Helsinki principles.

180

181   **Graphics**

182   Study design and assay workflow schematics were created with BioRender.com.

183

Results

BATTLE assay

We developed an assay workflow (**Figure 1a**) for the simultaneous detection of SARS-Cov-2 spike-specific T and B cells from cryopreserved PBMC. Cryopreserved PBMC were thawed and stimulated for 24 hours with overlapping peptide pools spanning SARS-CoV-2 spike to stimulate SARS-CoV-2 spike protein-reactive T cells, followed by incubation with fluorescent spike trimer tetramers to bait spike-binding B cells. These steps were followed by staining with fluorescent antibodies and viability dye prior to interrogation by flow cytometry or sorting. The gating strategy for flow cytometry is illustrated in **Supplementary Figure 1**. Using this approach, we were able to identify and quantify SARS-CoV-2 spike-reactive B cells (**Figure 1b**) in tandem with conventional activation-induced marker (AIM) T cell stimulation using as few as 3 x 10^6 PBMC per sample from SARS-CoV-2 mRNA vaccine recipients. Notably, stimulation with overlapping peptide pools did not interfere with the detection of antigen-specific B cells using fluorescent spike B cell probes (**Figure 1c, d**). Our results demonstrate that B And T cell Tandem Lymphocyte Evaluation (BATTLE) is an efficient assay capable of simultaneously quantifying and isolating antigen-specific B and T cells from a single PBMC sample.

Study design and serology

To demonstrate the utility of our new approach, we used the BATTLE assay to examine the impact of SARS-CoV-2 mRNA vaccination on spike protein-specific adaptive immunity following natural infection. We selected a cohort of subjects from a large study of convalescent plasma donors who experienced symptomatic but mild

207   infection and had a peripheral blood draw between 30 and 75 days of symptom

208   resolution (**Figure 2a**). This window was selected to capture the profile of antigen-

209   specific memory lymphocytes proximally to natural infection, but following resolution of

210   acute inflammatory responses to infection. We included subjects who were vaccinated

211   with two doses of mRNA vaccine at least 9 months following a negative SARS-CoV-2

212   PCR test and had a subsequent blood draw more than 30 days, but no more than 22

213   weeks following vaccination. These time constraints were chosen to ensure that

214   immune memory was stable prior to vaccination, and to capture the profile of antigen-

215   specific memory lymphocytes proximally to vaccination, but following resolution of acute

216   vaccine-driven inflammation.

217   To validate and extend the clinical utility of our findings, we evaluated the

218   serological profiles of each donor from the same visits used in the BATTLE assay. As

219   expected, IgG against the SARS-CoV-2 nucleocapsid protein, which is induced by

220   natural infection but not mRNA vaccination, declined between the first and post-

221   vaccination samples, while anti-N IgM was largely below the level of reliable detection

222   (**Figure 2b, c**). Serum anti-spike receptor-binding domain (RBD) IgG, but not IgM,

223   responses also were enhanced by mRNA vaccination (**Figure 2d, e**). Additionally, IgG,

224   but not IgM, raised against the spike receptor binding domain (RBD) from SARS-CoV-2

225   variant strains alpha and beta was significantly enhanced following mRNA vaccination,

226   although not all subjects had equally improved variant reactivity (**Supplementary**

227   **Figure 2**).

228   SARS-CoV-2 mRNA vaccination significantly increases the number and frequency of

229   spike-reactive B cells among peripheral blood B cells following natural infection.

230   To determine if SARS-CoV-2 mRNA vaccination had an impact on the B cell

231   response targeting spike protein, we examined spike-reactive B cells within post-

232   infection and post-infection plus vaccination PBMC samples. We observed a significant

233   increase in both the frequency and number of spike tetramer double-positive B cells in

234   post-vaccination samples, compared to natural infection alone (**Figure 3a, d,**

235   **Supplementary Figure 3a**). Importantly, spike-specific B cells were virtually absent in

236   PBMC samples collected prior to the onset of the SARS-CoV-2 pandemic,

237   demonstrating the specificity of the assay.

238   Taken together, our data are in alignment with other studies in which an

239   enhancement of spike-reactive adaptive B cell responses was observed in individuals

240   who received SARS-CoV-2 mRNA vaccination following natural infection (Wang et al.,

241   2021).

242   SARS-CoV-2 mRNA vaccination differentially impacts the spike-specific peripheral

243   CD4$^+$ and CD8$^+$ T cell compartments following natural infection.

244   We next sought to determine whether spike-reactive CD4$^+$ and CD8$^+$ T cells

245   within the same PBMC vial were similarly enhanced by mRNA vaccination after natural

246   SARS-CoV-2 infection. We quantified the expression of activation-induced markers on

247   these T cell subsets and found that, unlike for B cells targeting spike protein, the

248   frequency of CD4$^+$ spike peptide-activated T cells was not significantly enhanced

249   following mRNA vaccination compared to infection alone (**Figure 3b, e**). Although

250   significant changes were not observed for the full cohort, the frequency and number of

251   AIM$^+$ CD4$^+$ T cells was increased following vaccination for some individuals, particularly

252   for those with a lower initial spike-specific adaptive response. The same trend was

253   observed for subjects with low AIM$^+$ CD8$^+$ T cell frequencies following natural infection,

254   but unlike the spike-specific CD4$^+$ T cell compartment, CD8$^+$ T cells reactive to spike

255   were marginally enhanced in frequency following mRNA vaccination (**Figure 3c, f**). The

256   same patterns were present when adjusting for the number of cells used as input for the

257   assay, although for AIM$^+$ CD8$^+$ T cells differences between the groups no longer

258   reached statistical significance (**Supplementary Figure 3b, c**). As observed for spike-

259   specific B cells, few AIM$^+$ T cells were present in PBMC samples collected prior to the

260   onset of the SARS-CoV-2 pandemic, and unlike T cells from exposed subjects, those

261   from pre-SARS-CoV-2 samples were largely unresponsive to spike peptide pool

262   stimulation (**Supplementary Figure 3d, e**).

263   Correlative analysis of pooled data from both infection and infection plus

264   vaccination samples revealed a positive correlation between the frequency of SARS-

265   CoV-2 spike-specific B cells and serum IgG titers against the spike RBD from the

266   original Wuhan strain, as well as the alpha and beta variants (**Supplementary Figure**

267   **3f**). The frequency of AIM$^+$ CD8$^+$ T cells also positively correlated with anti-RBD IgG,

268   but this was only significant for the original SARS-CoV-2 strain. These results propose a

269   coordinated response to SARS-CoV-2 between B cells and CD8$^+$ T cells, potentially

270   without sustained synchronization with the CD4$^+$ T cell compartment. Taken together,

271   these data suggest that mRNA vaccination of previously-infected individuals influences

272   T cell subsets asymmetrically, and may allow those who mount a sub-optimal response

273   to infection to achieve an immunological setpoint not reached via natural infection.

274

Discussion

Here we demonstrate that B cells and CD4$^+$ and CD8$^+$ T cells specific for the same antigen can be simultaneously identified and quantified in a single PBMC sample. Furthermore, our results suggest that the ability for SARS-CoV-2 spike-specific B and T cells to be enhanced by mRNA vaccination following natural SARS-CoV-2 infection may not be equal. These findings also imply that the incorporation of additional antigens to SARS-CoV-2 vaccines may improve the balance of SARS-CoV-2-elicited memory. Other studies have demonstrated that the spike-specific B and T cell responses are highly heterogeneous within the human population (Dan et al., 2021; Rodda et al., 2020; Sette and Crotty, 2021; Weiskopf et al., 2020), findings which are echoed here. Our work suggests that despite this heterogeneity, trends in the patterns of antigen-specific B and T cell expansion and contraction can be detected even within small cohorts. Future work will examine whether the same level of heterogeneity exists for phenotypic and transcriptomic measures within the same populations.

Although our study was limited to the examination of PBMC, it is possible that these observations extend to other sources of lymphocytes, such as lymph node aspirates, bronchioalveolar lavage fluid, and bone marrow. Antigen-specific lymphocytes have been identified within these specimens in humans and non-human primates (Corbett et al., 2021; Kaneko et al., 2020; Turner et al., 2021), suggesting that BATTLE can be applied to maximize the yield of information gathered from these valuable samples.

Unlike other studies, we did not detect substantial frequencies or numbers of SARS-CoV-2 spike-binding T cells in non-exposed individuals (Grifoni et al., 2020;

298   Mateus et al., 2020). We attribute the disparity between our observations and others'

299   potentially to demographic variability between our sampling region and populations and

300   the those sampled in other studies. It is also possible that the sensitivity of our assay

301   was lower, although we consider this unlikely to be the case, as the quantities of

302   antigen-specific T cells we observed post-infection and post-vaccination were well-

303   aligned with those in the literature (Dan et al., 2021; Rydyznski Moderbacher et al.,

304   2020).

305   The observation of increased quantities of spike-specific B cells following mRNA

306   vaccination after natural infection supports the idea that mRNA vaccination is beneficial

307   even after natural adaptive immunity has developed. Additionally, our results suggest

308   that spike-reactive B cells may possess a capacity for vaccine-elicited expansion

309   beyond that of spike-reactive CD4$^+$ T cells. The mechanism by which this process may

310   occur is still an active area of investigation, but an attractive hypothesis is that B and T

311   cell populations each achieve an independent immunological setpoint following

312   resolution of acute infection or vaccine-induced activation. As the epitopes recognized

313   by B cells, CD4$^+$ T cells, and CD8$^+$ T cells, the timing and settings in which these events

314   occur, and the environmental signals these population receive can differ considerably, it

315   is tempting to speculate that uncoordinated dynamic expansion and contraction of B

316   and T cells can lead to the generation of immunological memory in a compartmentalized

317   manner. This interpretation would be supported with recent work describing coordinated

318   and timely B and T cell responses that lead to the generation of superior adaptive

319   immunity, and importantly that the lack thereof can have pathological consequences

320   (Lucas et al., 2021; Painter et al., 2021; Zohar et al., 2020). BATTLE is an ideal

321   approach that can be harnessed to explore these concepts.

322   Our study did not exclude the possibility that co-culture during T cell stimulation

323   and/or BCR baiting has an impact on each cell population at the transcriptional level.

324   Indeed, it will be important to examine the transcriptional signatures of T and B cells

325   isolated via BATTLE compared to traditional assays to explore this possibility. If the co-

326   stimulatory conditions do indeed cause activation or exhaustion of B or T cells, we

327   envision the adaptation of this assay to study the outcome of any resulting cognate

328   recognition-driven processes.

329   Given the paucity of antigen-specific memory lymphocytes following infection and

330   vaccination, the findings here have the potential to increase the breadth of diagnostic

331   and experimental protocols which rely on interrogation of these populations. Thus, our

332   studies have potential implications beyond the study of SARS-CoV-2 and mRNA

333   vaccination. We plan to adapt BATTLE to examine adaptive responses to additional

334   antigens in the future.

335   **Acknowledgements**

342 Terminal Histidine and Avi Tags, Recombinant from HEK293F Cells, NR-53524,

343 Peptide Array, SARS-Related Coronavirus 2 Spike (S) Glycoprotein, NR-52402, Spike

344 Glycoprotein Receptor Binding Domain (RBD) from SARS-Related Coronavirus 2,

345 United Kingdom Variant with C-Terminal Histidine Tag, Recombinant from HEK293

346 Cells, NR-54004, and Spike Glycoprotein Receptor Binding Domain (RBD) from SARS

347 Related Coronavirus 2, Beta Variant with C-Terminal Histidine Tag, Recombinant from

348 HEK293 Cells, NR-55278.

Contributions

350 K.L.N. conceptualized and executed experiments, analyzed the data, constructed

351 figures and wrote and edited the manuscript. M.W. aided in execution and analysis of

352 serum ELISAs. S.J.T. and T. P.E. contributed to project administration and funding

353 acquisition. A.T.W. conceptualized experiments, and aided in the analysis of data,

354 project administration, funding acquisition, and the writing and review of the manuscript.

355 All authors participated in final review of the manuscript.

Competing financial interests

357 S.J.T. reports compensation from Pfizer, during the conduct of the study; personal fees

358 from Merck, Sanofi, Takeda, Themisbio, and Janssen, outside the submitted work. All

359 other authors declare that the research was conducted in the absence of any

360 commercial or financial relationships that could be construed as a potential conflict of

361 interest.

Data Availability

363 Flow cytometry data has been submitted under ID FR-FCM-Z4PB and annotated at

364 http://flowrepository.org. All other data is available upon request.

365

Figure Legends

Figure 1: BATTLE: B and T Tandem Lymphocyte Evaluation.

A: Schematic of BATTLE assay workflow.

B: Representative flow cytometry plot of SARS-CoV-2 spike protein-specific B cells detected from the PBMC of a vaccinated individual using the BATTLE assay. Pre-gating is shown above the plot. The frequency of cells within the double-positive gate among B cells is shown inside the gate.

C-D: Total (purple) or monocyte-depleted (teal) PBMC from SARS-CoV-2 mRNA vaccinated individuals were stimulated with overlapping spike peptide pools or DMSO alone and baited with dual spike BCR probes. The frequency among B cells (C) and number per 1 x 10^6 cells plated (D) of B cells positive for both probes are shown, with each dot representing an individual. Paired DMSO control and peptide pool-stimulated samples from the same individual are connected by a solid line. Paired groups were analyzed by Mann-Whitney U test (n = 5, exact two-tailed p > 0.9999 (C), p = 0.6905 (D)).

Figure 2: Study design and serology.

A: Timeline of SARS-CoV-2 convalescent study and sample collection.

B-E: Paired sera following natural infection and after subsequent vaccination from the same individual were assessed for IgM and IgG binding to SARS-CoV-2 nucleocapsid (B, C) or spike RBD (D, E) proteins. Each dot color represents an individual and pairs are connected by a solid line. Differences between infection and infection + vaccination groups were analyzed by Wilcoxon matched-pairs

389   signed rank test (n = 9, exact two-tailed p > 0.9999 (B), p = 0.0078, 0.2500,

390   0.0039 (C-E)).

391

392   **Figure 3: Spike-specific lymphocyte responses following natural infection and**

393   **subsequent vaccination.**

394   A-C: Representative flow cytometry plots of SARS-CoV-2 spike protein-specific B

395   cells (A), OX40/CD69$^+$ CD4$^+$ (B) and CD25/CD69$^+$ CD8$^+$ (C) T cells detected

396   from PBMC using the BATTLE assay from a sample collected independently

397   prior to the onset of the pandemic, and following natural infection and

398   subsequent vaccination in the same individual (left to right, respectively). Pre-

399   gating is shown above each panel. The frequency of cells within the double-

400   positive gate among B cells, CD4+ T cells, and CD8+ T cells is shown inside the

401   gates, respectively.

402   D: The frequency among B cells of cells positive for both probes are shown, with

403   each dot or dot pair representing an individual. Paired post-infection and post-

404   infection plus vaccination samples from the same individual are connected by a

405   solid line. Paired groups were analyzed by Wilcoxon matched-pairs signed rank

406   test (n = 9, exact two-tailed p = 0.0039).

407   E: The frequency among CD4$^+$ T cells of cells positive for activation-induced

408   markers OX40 and CD69 are shown, following subtraction of DMSO control

409   values. Each dot or dot pair represents an individual. Paired post-infection and

410   post-infection plus vaccination samples from the same individual are connected

411   by a solid line. Paired groups were analyzed by Wilcoxon matched-pairs signed

412   rank test (n = 9, exact two-tailed p > 0.9999).

413   F: The frequency among CD8$^+$T cells of cells positive for activation-induced markers

414   CD25 and CD69 are shown, following subtraction of DMSO control values. Each

415   dot or dot pair represents an individual. Paired post-infection and post-infection

416   plus vaccination samples from the same individual are connected by a solid line.

417   Paired groups were analyzed by Wilcoxon matched-pairs signed rank test (n = 9,

418   exact two-tailed p = 0.0234).

419   **Supplementary Figure 1: BATTLE assay gating strategy.**

420   The flow cytometry gating strategy used to identify SARS-CoV-2 spike protein-

421   specific B and T cells is shown using a representative sample.

422   **Supplementary Figure 2: SARS-CoV-2 variant spike RBD serology.**

423   A-D: Paired sera following natural infection and after subsequent vaccination from

424   the same individuals were assessed for IgM and IgG binding to SARS-CoV-2

425   alpha (A, B) or beta (C, D) variant spike RBD proteins. Each dot color represents

426   an individual and pairs are connected by a solid line. Differences between

427   infection and infection + vaccination groups were analyzed by Wilcoxon matched-

428   pairs signed rank test (n = 9, exact two-tailed p = 0.6250, 0.0195, 0.3125, 0.0469

429   (A-D)).

430   **Supplementary Figure 3: AIM$^+$ T cell analysis and correlative analysis.**

431   A: The number of B cells positive for both probes per 1 x 10^6 cells plated for

432   stimulation is shown, with each dot or dot pair representing an individual. Paired

433   post-infection and post-infection plus vaccination samples from the same

434 individual are connected by a solid line. Paired groups were analyzed by

435 Wilcoxon matched-pairs signed rank test (n = 9, exact two-tailed p = 0.0039).

436 B: The number of CD4$^+$ T cells positive for activation-induced markers OX40 and

437 CD69 per 1 x 10^6 cells plated for stimulation is shown, following subtraction of

438 DMSO control values. Each dot or dot pair represents an individual. Paired post-

439 infection and post-infection plus vaccination samples from the same individual

440 are connected by a solid line. Paired groups were analyzed by Wilcoxon

441 matched-pairs signed rank test (n = 9, exact two-tailed p = 0.5703).

442 C: The number of CD8$^+$ T cells of cells positive for activation-induced markers CD25

443 and CD69 are shown, following subtraction of DMSO control values. Each dot or

444 dot pair represents an individual. Paired post-infection and post-infection plus

445 vaccination samples from the same individual are connected by a solid line.

446 Paired groups were analyzed by Wilcoxon matched-pairs signed rank test (n = 9,

447 exact two-tailed p = 0.2500).

448 D. The frequency of AIM$^+$ CD4$^+$ T cells among total CD4$^+$ T cells is shown with each

449 pair of dots representing an individual. Paired DMSO control and peptide pool-

450 stimulated samples from the same individual are connected by a solid line (n = 4

451 pre-SARS-CoV-2, 20 post-SARS-CoV-2). Subjects exposed to SARS-CoV-2

452 mRNA vaccination only (turquoise), natural infection only (purple), and infection

453 plus vaccination (orange) are shown.

454 E. The frequency of AIM$^+$ CD8$^+$ T cells among total CD8$^+$ T cells is shown with each

455 pair of dots representing an individual. Paired DMSO control and peptide pool-

456 stimulated samples from the same individual are connected by a solid line (n = 4

457   pre-SARS-CoV-2, 20 post-SARS-CoV-2). Subjects exposed to SARS-CoV-2

458   mRNA vaccination only (turquoise), natural infection only (purple), and infection

459   plus vaccination (orange) are shown.

460   F. Spearman's rho rank correlation coefficients are graphed by circle color according

461   to the scale on the right of the panel. The size of the circle indicates increasing

462   statistical significance. Correlation matrix was generated from data as presented

463   in the previous figures representing the combined SARS-CoV-2 infection and

464   vaccination-elicited immune response.

465

466   **Supplementary Table 1: Fluorescent antibodies used in BATTLE assay.**

467

468   **References**

469   Altman, J.D., Moss, P.A., Goulder, P.J., Barouch, D.H., McHeyzer-Williams, M.G., Bell,
470   J.I., McMichael, A.J., and Davis, M.M. (1996). Phenotypic analysis of antigen-specific T
471   lymphocytes. Science *274*, 94–96.

472   Boonyaratanakornkit, J., and Taylor, J.J. (2019). Techniques to Study Antigen-Specific
473   B Cell Responses. Front. Immunol. *10*, 1694.

474   Corbett, K.S., Nason, M.C., Flach, B., Gagne, M., O'Connell, S., Johnston, T.S., Shah,
475   S.N., Edara, V.V., Floyd, K., Lai, L., et al. (2021). Immune correlates of protection by
476   mRNA-1273 vaccine against SARS-CoV-2 in nonhuman primates. Science *373*,
477   eabj0299.

478   Czerkinsky, C.C., Nilsson, L.A., Nygren, H., Ouchterlony, O., and Tarkowski, A. (1983).
479   A solid-phase enzyme-linked immunospot (ELISPOT) assay for enumeration of specific
480   antibody-secreting cells. J. Immunol. Methods *65*, 109–121.

481   Dan, J.M., Lindestam Arlehamn, C.S., Weiskopf, D., da Silva Antunes, R., Havenar-
482   Daughton, C., Reiss, S.M., Brigger, M., Bothwell, M., Sette, A., and Crotty, S. (2016). A
483   Cytokine-Independent Approach To Identify Antigen-Specific Human Germinal Center T
484   Follicular Helper Cells and Rare Antigen-Specific CD4+ T Cells in Blood. J. Immunol.
485   Baltim. Md 1950 *197*, 983–993.

486   Dan, J.M., Mateus, J., Kato, Y., Hastie, K.M., Yu, E.D., Faliti, C.E., Grifoni, A., Ramirez,
487   S.I., Haupt, S., Frazier, A., et al. (2021). Immunological memory to SARS-CoV-2
488   assessed for up to 8 months after infection. Science *371*, eabf4063.

489   Fang, H., Wegman, A.D., Ripich, K., Friberg, H., Currier, J.R., Thomas, S.J., Endy, T.P.,
490   and Waickman, A.T. (2021). Persistent COVID-19 Symptoms Minimally Impact the
491   Development of SARS-CoV-2-Specific T Cell Immunity. Viruses *13*, 916.

492   Frentsch, M., Arbach, O., Kirchhoff, D., Moewes, B., Worm, M., Rothe, M., Scheffold,
493   A., and Thiel, A. (2005). Direct access to CD4+ T cells specific for defined antigens
494   according to CD154 expression. Nat. Med. *11*, 1118–1124.

495   Grifoni, A., Weiskopf, D., Ramirez, S.I., Mateus, J., Dan, J.M., Moderbacher, C.R.,
496   Rawlings, S.A., Sutherland, A., Premkumar, L., Jadi, R.S., et al. (2020). Targets of T
497   Cell Responses to SARS-CoV-2 Coronavirus in Humans with COVID-19 Disease and
498   Unexposed Individuals. Cell *181*, 1489-1501.e15.

499   Julius, M.H., Masuda, T., and Herzenberg, L.A. (1972). Demonstration that antigen-
500   binding cells are precursors of antibody-producing cells after purification with a
501   fluorescence-activated cell sorter. Proc. Natl. Acad. Sci. U. S. A. *69*, 1934–1938.

502   Kaneko, N., Kuo, H.-H., Boucau, J., Farmer, J.R., Allard-Chamard, H., Mahajan, V.S.,
503   Piechocka-Trocha, A., Lefteri, K., Osborn, M., Bals, J., et al. (2020). Loss of Bcl-6-

504 Expressing T Follicular Helper Cells and Germinal Centers in COVID-19. Cell
505 S0092867420310679.

506 Kern, F., Faulhaber, N., Frömmel, C., Khatamzas, E., Prösch, S., Schönemann, C.,
507 Kretzschmar, I., Volkmer-Engert, R., Volk, H.-D., and Reinke, P. (2000). Analysis of
508 CD8 T cell reactivity to cytomegalovirus using protein-spanning pools of overlapping
509 pentadecapeptides. Eur. J. Immunol. *30*, 1676–1682.

510 Lucas, C., Klein, J., Sundaram, M.E., Liu, F., Wong, P., Silva, J., Mao, T., Oh, J.E.,
511 Mohanty, S., Huang, J., et al. (2021). Delayed production of neutralizing antibodies
512 correlates with fatal COVID-19. Nat. Med. *27*, 1178–1186.

513 Maecker, H.T., Dunn, H.S., Suni, M.A., Khatamzas, E., Pitcher, C.J., Bunde, T.,
514 Persaud, N., Trigona, W., Fu, T.-M., Sinclair, E., et al. (2001). Use of overlapping
515 peptide mixtures as antigens for cytokine flow cytometry. J. Immunol. Methods *255*, 27–
516 40.

517 Mateus, J., Grifoni, A., Tarke, A., Sidney, J., Ramirez, S.I., Dan, J.M., Burger, Z.C.,
518 Rawlings, S.A., Smith, D.M., Phillips, E., et al. (2020). Selective and cross-reactive
519 SARS-CoV-2 T cell epitopes in unexposed humans. Science eabd3871.

520 Moody, M.A., and Haynes, B.F. (2008). Antigen-specific B cell detection reagents: use
521 and quality control. Cytom. Part J. Int. Soc. Anal. Cytol. *73*, 1086–1092.

522 Newell, K.L., Clemmer, D.C., Cox, J.B., Kayode, Y.I., Zoccoli-Rodriguez, V., Taylor,
523 H.E., Endy, T.P., Wilmore, J.R., and Winslow, G.M. (2021). Switched and unswitched
524 memory B cells detected during SARS-CoV-2 convalescence correlate with limited
525 symptom duration. PloS One *16*, e0244855.

526 Painter, M.M., Mathew, D., Goel, R.R., Apostolidis, S.A., Pattekar, A., Kuthuru, O.,
527 Baxter, A.E., Herati, R.S., Oldridge, D.A., Gouma, S., et al. (2021). Rapid induction of
528 antigen-specific CD4+ T cells is associated with coordinated humoral and cellular
529 immunity to SARS-CoV-2 mRNA vaccination. Immunity *54*, 2133-2142.e3.

530 Rodda, L.B., Netland, J., Shehata, L., Pruner, K.B., Morawski, P.M., Thouvenel, C.,
531 Takehara, K.K., Eggenberger, J., Hemann, E.A., Waterman, H.R., et al. (2020).
532 Functional SARS-CoV-2-specific immune memory persists after mild COVID-19
533 (Infectious Diseases (except HIV/AIDS)).

534 Rydyznski Moderbacher, C., Ramirez, S.I., Dan, J.M., Grifoni, A., Hastie, K.M.,
535 Weiskopf, D., Belanger, S., Abbott, R.K., Kim, C., Choi, J., et al. (2020). Antigen-
536 Specific Adaptive Immunity to SARS-CoV-2 in Acute COVID-19 and Associations with
537 Age and Disease Severity. Cell *183*, 996-1012.e19.

538 Sette, A., and Crotty, S. (2021). Adaptive immunity to SARS-CoV-2 and COVID-19. Cell
539 *184*, 861–880.

540   Turner, J.S., Kim, W., Kalaidina, E., Goss, C.W., Rauseo, A.M., Schmitz, A.J., Hansen,
541   L., Haile, A., Klebert, M.K., Pusic, I., et al. (2021). SARS-CoV-2 infection induces long-
542   lived bone marrow plasma cells in humans. Nature *595*, 421–425.

543   Wang, Z., Muecksch, F., Schaefer-Babajew, D., Finkin, S., Viant, C., Gaebler, C.,
544   Hoffmann, H.-H., Barnes, C.O., Cipolla, M., Ramos, V., et al. (2021). Naturally
545   enhanced neutralizing breadth against SARS-CoV-2 one year after infection. Nature
546   *595*, 426–431.

547   Weiskopf, D., Schmitz, K.S., Raadsen, M.P., Grifoni, A., Okba, N.M.A., Endeman, H.,
548   van den Akker, J.P.C., Molenkamp, R., Koopmans, M.P.G., van Gorp, E.C.M., et al.
549   (2020). Phenotype and kinetics of SARS-CoV-2-specific T cells in COVID-19 patients
550   with acute respiratory distress syndrome. Sci. Immunol. *5,* eabd2071.

551   Zohar, T., Loos, C., Fischinger, S., Atyeo, C., Wang, C., Slein, M.D., Burke, J., Yu, J.,
552   Feldman, J., Hauser, B.M., et al. (2020). Compromised Humoral Functional Evolution
553   Tracks with SARS-CoV-2 Mortality. Cell *183*, 1508-1519.e12.

554
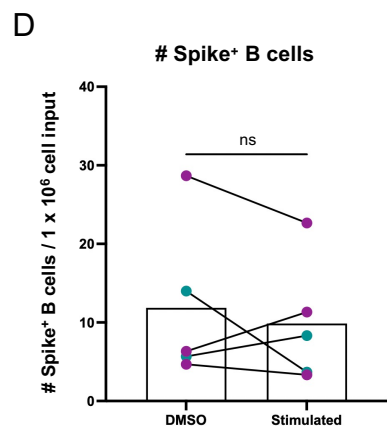
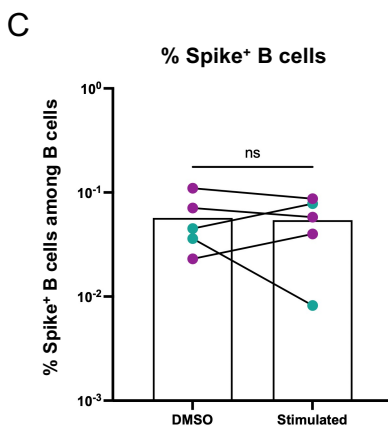**Fig. 1: BATTLE: B And T Tandem Lymphocyte Evaluation**

A

Cryopreserved PBMC → 24 hr. Spike peptide stimulation → 1 hr. incubation with dual spike probes → 30 min. surface stain + 30 min. viability stain → Quantification of spike-specific B & T lymphocytes

B

Live, CD14/CD56⁻, CD3⁻ **CD19⁺**

Spike probe BV-421

0.087

Spike probe APC

C

% Spike⁺ B cells

% Spike⁺ B cells among B cells

ns

DMSO   Stimulated

D

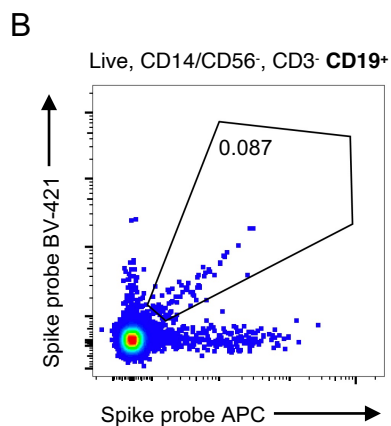**# Spike⁺ B cells**

Spike⁺ B cells / 1×10^6 cell input

ns

DMSO   Stimulated

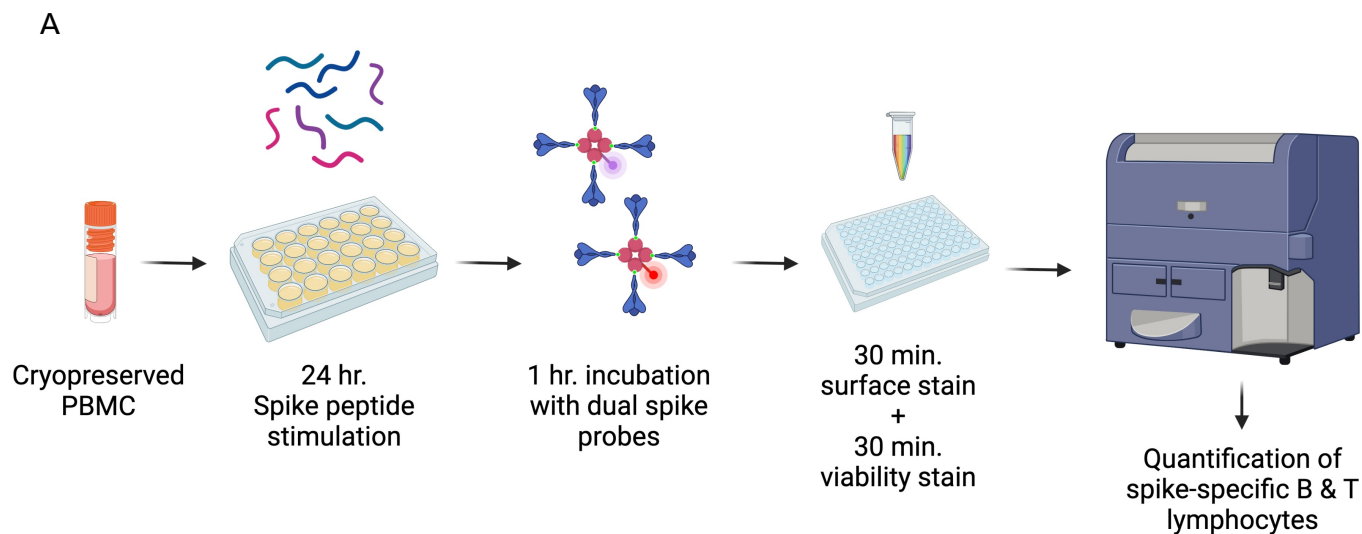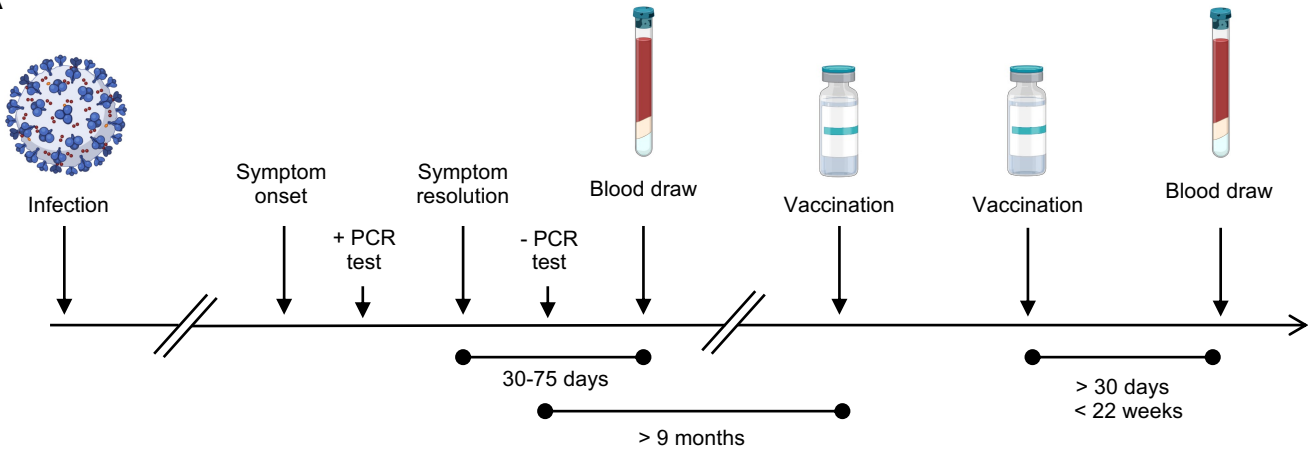**Fig. 2: Study design and serology**

A

B — **Anti-N IgM** — ns

C — **Anti-N IgG** — **

D — **Anti-RBD IgM** — ns

E — **Anti-RBD IgG** — **

EC$_{50}$ Kd

Infection   Infection + Vax
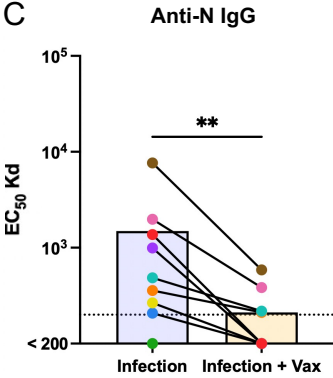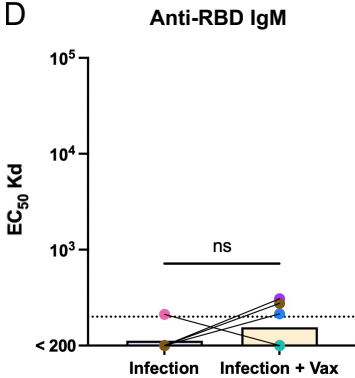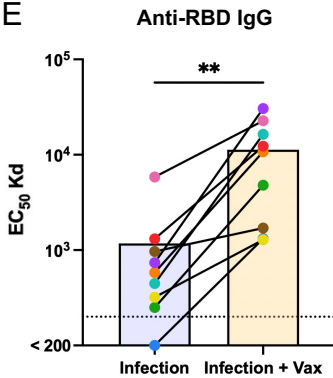
Fig. 3 Spike-specific lymphocyte responses following natural infection and subsequent vaccination

A Live, CD14/CD56-, CD3- **CD19+**

Pre-SARS-CoV-2 | Natural infection | Infection + Vaccination
0.003 | 0.043 | 0.17

Spike probe BV-421
Spike probe APC

B Live, CD14/CD56-, CD19- CD3+ CD8- **CD4+**

Pre-SARS-CoV-2 | Natural infection | Infection + Vaccination
0.031 | 1.69 | 2.04

OX40 FITC
CD69 BV-785

C Live, CD14/CD56-, CD19- CD3+ CD4- **CD8+**

Pre-SARS-CoV-2 | Natural infection | Infection + Vaccination
0.015 | 0.21 | 0.43

CD25 APC-Cy7
CD69 BV-785

D % Spike+ B cells
% Spike+ B cells among B cells
**
Pre-SARS-CoV-2, Infection, Infection + Vax

E % AIM+ CD4+ T cells
% CD69+ OX40+ among CD4+ T cells
ns
Pre-SARS-CoV-2, Infection, Infection + Vax

F % AIM+ CD8+ T cells
% CD69+ CD25+ among CD8+ T cells
*
Pre-SARS-CoV-2, Infection, Infection + Vax